

Heat transfer performance of stainless steel, mild steel and aluminium target plate for various configurations of impinging air jet

K. Jeyajothi, P. Kalaichelvi*

Department of Chemical Engineering, National Institute of Technology, Tiruchirappalli-620015, Tamil Nadu, India

Received, July 17, 2018; Revised, August 3, 2018

In spite of several studies carried out on jet impingement on a plane surface, this work describes a new approach of comparing the heat transfer characteristics when three different materials are used as a target. The heated target plates are made up of stainless steel, mild steel and aluminium and are kept at different heights (2 to 8 mm) from a nozzle with diameter ranging from 0.5 to 3 mm. Measurements were done at the stagnation point using air jets with velocity of 6.4 and 9.2 m/s. The major characteristics of a jet impinging on a plane could be shown by straightforward experiments like spreading over method. Nusselt number was calculated for various values of jet Reynolds number and it was observed that adequate cooling of the plate is attained and enhanced with an increase in Reynolds number. It was also noted that the placement of the target is critical for optimum performance in practical applications. The increment in air velocity and Reynolds number improved heat transfer while increment in nozzle height decreased the performance at the stagnation point. Furthermore, three new reliable empirical correlations were established using the experiments performed.

Keywords: Impinging air jet, Target plate material, Round nozzle, Stagnation Nusselt number, Empirical correlation.

INTRODUCTION

Impinging jets, which are gas or liquid released with specific flow direction towards or over a target surface, provide efficient means for energy and mass transfer in many modern industrial processes. Some heat transfer applications of impinging jets includes stock material cooling, electronic components cooling, material forming, defogging of heated optical surfaces, internal cooling of turbine blades, heat treatment and cooling of critical machine parts [1]. They can be found in equipment involving heating, cooling or drying units, pulverisation, food processing, annealing of materials, building ventilation and cleaning operations. Removal of small particulates from surfaces and drying are some typical examples for mass transfer applications. Heat transfer due to impingement and abrasion caused due to landing and take-off jet devices were also studied [2–4].

The mechanism and structure of impinging jets should be understood to find the suitable methods of predicting jet performance. Optimized design of these kinds of installations need in-depth idea on the jet structure. Two-dimensional incompressible laminar slot air jet impingement on isothermally heated surface was studied for $100 \leq \text{Re}_D \leq 400$ with different ratios of separation distance (nozzle-to-target plane distance) and jet width ranging from 1 to 8 mm to develop correlations between boundary layer thickness and

stagnation Nusselt number (Nu_s) with respect to Re_D and separation distance [5]. Another experimental study of heat transfer behaviour of a confined slot laminar jet impingement has been performed for $190 \leq \text{Re}_D \leq 1537$ [6]. Investigation on the rate of cooling of a surface, due to the effect of multi-jet array, revealed an intense periodic oscillation in the Nusselt number (Nu) streamwise profile for different array spacing when the distance between the target plate and jet is fixed [7]. The peak in heat transfer coefficient increased by keeping smaller jet-to-plate spacing and diminished at larger spacing when the jet applied was cross flow [8]. In studies on an impinging square jet through cross flow, formation of vortices was noticed and their number, strength and location depended on the jet-to-cross flow velocity and on the jet-to-plate spacing [9]. Operation of jet at cross flow also has been reported to reduce Nu by 60% [10]. Protrusions on the confinement surface restricted the jet inlet interaction with exhaust flow while enhancing heat transfer rates [11]. Studies on various other types of jets including elliptical jets, liquid jets and isothermal gas and flame jets were also reported [12–14]. Apart from experimental works, theoretical or empirical analysis and various types of computational methods were applied for studying impinging jets [15–17].

The main goal of the study is to determine and suggest the best performing plate material for achieving the best heat transfer characteristics out of

* To whom all correspondence should be sent:
E-mail: kalai@nitt.edu

the three selected target plates labelled as SS (stainless steel), MS (mild steel) and AL (aluminium). No such comparison of heat transfer characteristics of target material for impinging air jet was found in the literature and this work is the first attempt in that aspect. Operating configuration was optimized using different input parameters like air jet velocities, nozzle diameters, nozzle heights from target surface and Reynolds number and the outcome performance was measured in terms of Nu. Only few studies were performed on analysis of the combined effect of such input parameters. Therefore, this study would be a significant contribution to the heat transfer research on the air jet impingement.

Only stagnation point was considered for this study because our preliminary studies at different locations determining stagnation, local and average heat transfer coefficients showed that at the stagnation point, a maximum heat transfer occurred giving high Nu (data not shown). This study intended: (1) to examine the flow properties of the jet; (2) to explore the effect of Reynolds number and nozzle distance from stagnation point; (3) to develop empirical correlation of Nu_s for all three materials and (4) to validate the results from experiments with the theoretical values.

EXPERIMENTAL

Experimentation setup

The setup used for the experimentation consisted of three major components, viz., air supply system, heated target plate and monitoring instrumentation.

Fig. 1 elucidates the schematics of the major components of the setup. The working fluid (air) is compressed through the compressor (CEC model A829, 7 kg/cm², 760 rpm, 120 L capacity with single-phase induction motor, Prv-15 model pressure with air filters, regulator, bypass valve and a pressure gauge with 0-14 kg/cm² range). Then, the air is passed through a flowmeter (RG-05 model glass tube rotameter with pressure rating of 40 bar and range 0-100 Lpm) to a flexible tube at the end of the air supply system which is connected to a duct and a round-edged nozzle is fitted to this duct. As per the experimental configuration, the nozzle with corresponding dimension is used at the end of the duct. A Kapton heater (vari-volt type 10-p capacity 10A) with a uniform heating element (3950 W/m²) inserted in an insulator assembly was used to heat the target plate. The power supplied was monitored by employing a voltmeter, measuring the potential difference and an ammeter, measuring the current flow. A digital anemometer (Lutron model: AM-4201) and a mercury thermometer were used to measure the air jet velocity and temperature, respectively. The target was placed perpendicularly to the axis of the impinging jet. The spacing height between the nozzle and the plate was adjusted by a moving support, which facilitated vertical and horizontal movements. The air jet from the nozzle impinged normally onto the center of the heated target and a precisely calibrated K-type thermocouple was used to record the plate surface temperature.

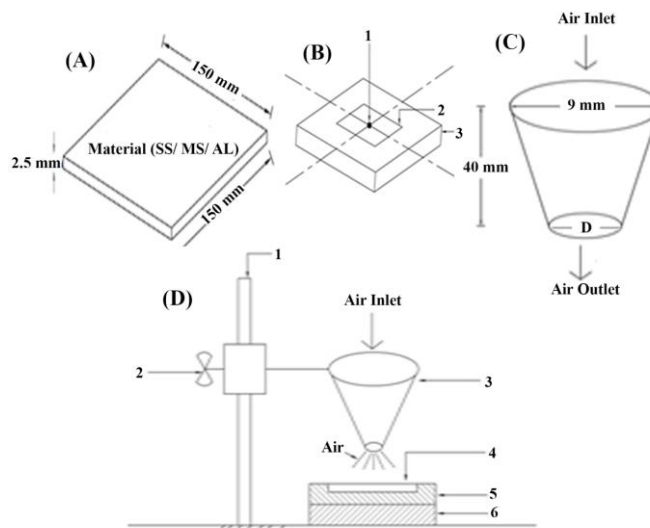


Fig. 1. (A) Target plate (B) Plate insulator heater box [1–Stagnation point, 2–Target plate, 3–Fire brick chamber with Kapton heater] (C) Nozzle element [D–0.5 to 3 mm] (D) Experimental arrangement [1–Stand, 2–Height adjusting clamp, 3–Jet nozzle, 4–Target surface, 5–Heating chamber, 6–Base]

$$Re_D = \frac{D \times v \times \rho}{\mu} \quad (1)$$

Experiments were carried out for different nozzle diameters (D) and various nozzle-to-plate distances at two air flow velocities (v) (as shown in Table. 1). The air supply from the compressor was controlled by the flowmeter to vary the air velocity. Heating by the heater and cooling due to impinging jet occurred simultaneously. A steady state condition was achieved when the heat loss by convection from the top surface of the plate equals the heat conducted to the top surface of the heated plate. After the steady state was achieved for 45 min, the surface temperature of the plate was recorded. A total of 108 measurements were made with the thermocouple installed for measuring the local temperatures of the heated target surface. The measurements for all experiments were performed in a symmetric mode and the acquisition of all experimental data was at a steady state. The configuration used in this study is compared to some of the impinging jet configurations from the existing literature in Table 2.

Estimation of heat transfer characteristics

The characteristics of heat transfer were deduced by converting the temperature data into heat transfer information. The stagnation heat transfer coefficients were determined to calculate the removal of heat from the test surface and to obtain an accurate convective heat flux [6]. Reynolds number was calculated with the air flow parameters using Eq. 1.

where, μ is the viscosity of air; ρ is the density of air.

At the steady state conditions, the stagnation heat transfer coefficient (h_s) was derived for the plate with thickness of 2.5 mm at the center of the plate (i.e., distance (x) from the target plate center = 0). By combining the Fourier's law with the Newton's law of cooling (Eq. 2), the local convective heat transfer at the stagnation point was derived by Eq. 3 and the stagnation Nusselt number (Nu_s) was calculated from Eq. 4.

$$-KA \left. \frac{dT}{dx} \right|_{x=2.5} = hA (T_w - T_a) \quad (2)$$

$$h_s = \frac{2.5 \times q}{(T_{w,x} - T_a)} \quad (3)$$

where, A is the surface area of the plate; K is the thermal conductivity of air; $T_{w,x}$ is the temperature of the wall at a distance x; T_a is the temperature of the air; T_w is the temperature of the wall; h is the heat transfer coefficient; q is the convective heat flux on the top of the plate.

$$Nu_s = \frac{h_s \times D}{K} \quad \text{at } x=0 \quad (4)$$

Table 1. Operational parameters

Parameter	Range
Nozzle diameter	0.5, 1.0, 1.5, 2.0, 2.5 and 3.0 mm
Height of nozzle above the plate	2, 4 and 8 mm
Air velocity	6.4 and 9.2 m/s
Reynolds number	192.61 to 1661.26
Target plate thickness	2.5 mm

Table 2. Comparison of experimental configurations

References	D (mm)	H/D	Re_D	Nozzle geometry	Target plate
Chou and Hung [5]	1, 1.5	1-8	100-400	RN	SS
Lin <i>et al.</i> [6]	5	1-20	190-1537	OP	SS
Rady and Arquis [11]	1, 1.5	1-4	250, 500	CN	SS
Arjocu and Liburdy [12]	0.5, 1.5	1-6	300, 1500	SA	AL
Morris <i>et al.</i> [13]	3.18, 6.35	1-4	8500-13000	CN	SS
Meola [21]	2-12	1.6-20	200-100000	RN, RectO	SS
Mahgoub [22]	2.7-11	11	$10^5 - 10^6$	RectO	AL
Present study	0.5-3	0.67-16	192.61-1661.26	R-LTN	SS,MS,AL

Abbreviations: SA=square array, OP=jet orifice plate, R-LTN=round long-throat nozzle, CN= circular nozzle, RN=round nozzle, RectO=rectangular opening, SS=stainless steel, MS=mild steel, AL=aluminium

The uncertainty in Nusselt number was predisposed mostly by the determination of heat flux and wall temperature. The surface heat flux was affected by the difference in the plate dimensions that was claimed in the supplier description to be less than $\pm 7\%$ of the normal value. The uncertainty in the values measured by a calibrated flow meter was $\pm 0.5\%$ and that of the thermocouple was $\pm 0.75\%$. The Nusselt number uncertainty was acknowledged to be optional and stretched from 4.5 to 10.43% [18]. Thus, the cumulative uncertainty was found to be $< 9\%$, which is well within the acceptable limits ($\pm 15\%$) [14,19] in experimental data.

RESULTS AND DISCUSSION

The foremost inflection of the present study is heat transfer characteristics at the stagnation point of an unconfined jet on three different target materials. A sequence of experimental trials was conducted to discover the flow and heat transfer characteristics with the selected jet configurations having three different nozzle heights (H) above the plate for each plate material. This set of experiments was repeated with each of the 6 nozzles (with $D = 0.5$ to 3 mm) leading to 54 performance outcomes for each of the two air velocities. The effect of nozzle height or nozzle-to-plate distance on Nu_S for the various nozzle diameters is compared in Figs. 2 and 3 for the three target materials (SS, MS and AL), where $v = 6.4$ and 9.2 m/s, respectively. It is seen that the Nu_S increased with increase in the velocity for every nozzle, while the Nu_S decreased as the height increased. The decrease in Nu_S was more rapid when H was increased from 2 to 4 mm. This may be mainly due to the reduction of air flow as the distance between nozzle and plate was increased [6]. This effect was witnessed because of higher air flow dispersion. At lower height, the air flow was confined at the impinging point and hence, the heat transfer was higher at lower heights. Therefore, the height with maximum heat transfer (2 mm) was considered for further calculations. Among the three materials, SS showed high Nu_S values while AL had the least Nu_S values. When $H \leq 4$ mm, the Nu_S of the materials were close to each other for $D \leq 1.5$ mm. As D increased above 1.5 mm, SS and MS had nearer Nu_S , and AL had a notably lower Nu_S . Thus, the low heat transfer ability of AL is clearly evident. The Reynolds number varies according to nozzle

diameter and the air jet velocities on which it is dependent. Re_D values calculated for this study ranged from laminar to transient regime. The effects of Re_D on Nu_S when $H = 2$ mm and $v = 9.2$ m/s were compared for the target materials in Fig. 4, which reveals that the Nu_S values were higher for higher Re_D . As the Re_D increased, the Nu_S distribution became slightly convex. The comparable trend of increase or decrease in the Nu_S with change of materials was perceptible. It is further inferred that the bigger the nozzle diameter, the higher is Nu_S because of the higher Re_D associated with the larger nozzles [6]. Moreover, the smaller nozzle could have delivered a lower quantity of air compared to that of the bigger nozzle. This, in turn, has affected the Nu_S and subsequently, the heat transfer characteristics. Flow resistance with the smaller nozzle was yet another factor affecting the Nu_S .

The heat transfer coefficient condensed in dimensionless form as Nu could be related to the Reynolds number according to Eq. 5 [20], which conveys that the ratio of total heat transfer corresponding to conductive heat transfer is proportional to the momentum flux:

$$Nu \propto Re_D^\alpha \quad (5)$$

where, α is the power law constant and its value ranges from 0.5 to 0.99 in the experiments depending on the range of Reynolds number.

Meola [21] and Mahgoub [22] investigated various power law equations at the stagnation zone and stated that the Nusselt numbers could be correlated in the following form:

$$Nu = C_1 Re_D^{C_2} \quad (6)$$

where, C_1 and C_2 are empirical constants obtained from experimental data. In particular, the heat transfer near to the stagnation point may be computed according to Eq. 6 for the laminar and transient regime ($276.88 \geq Re_D \leq 1661.26$ at a velocity of 9.2 m/s) by calculating the correlation factors from Fig. 4 for all 3 materials, and the data sets are reduced to Eqs.7 (SS), 8 (MS) and 9 (AL). Their corresponding correlation coefficient (R^2) values are 0.995, 0.993 and 0.961, respectively.

$$Nu_S = 0.425 Re_D^{0.892} \quad (7)$$

$$Nu_S = 0.393 Re_D^{0.891} \quad (8)$$

$$Nu_S = 0.527 Re_D^{0.805} \quad (9)$$

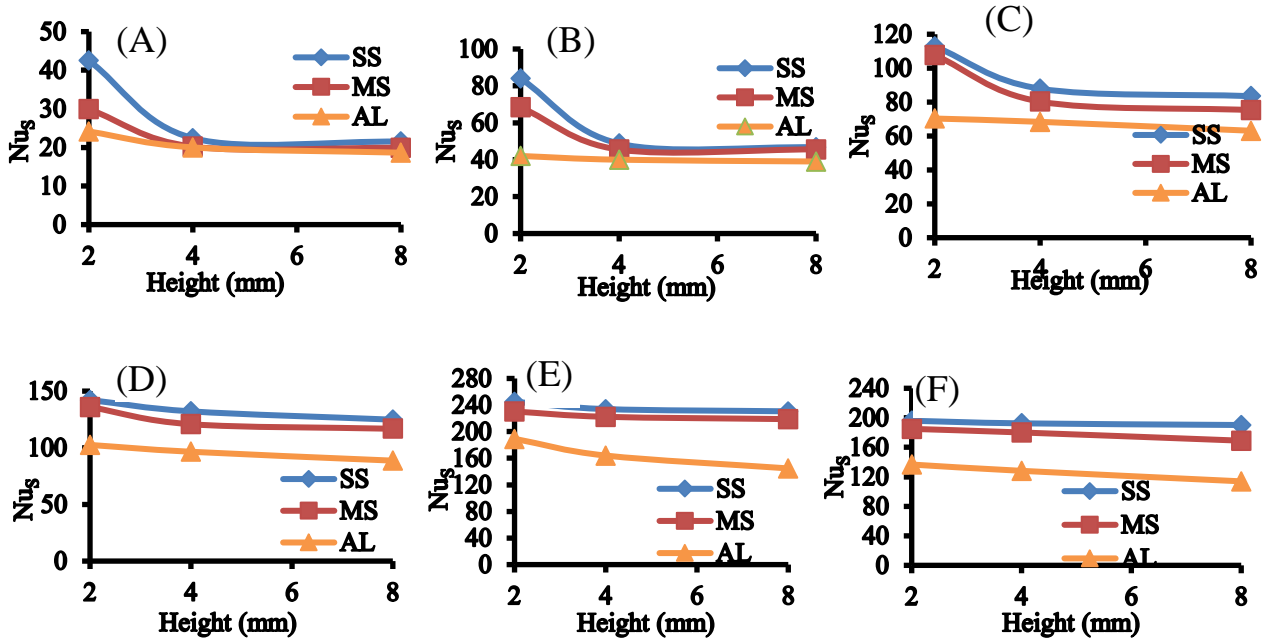


Fig. 2. Effect of nozzle height (H) on the Nu_s at air velocity (v) of 6.4 m/s for various nozzle diameters (A) 0.5 mm; (B) 1 mm; (C) 1.5 mm; (D) 2 mm; (E) 2.5 mm; (F) 3 mm

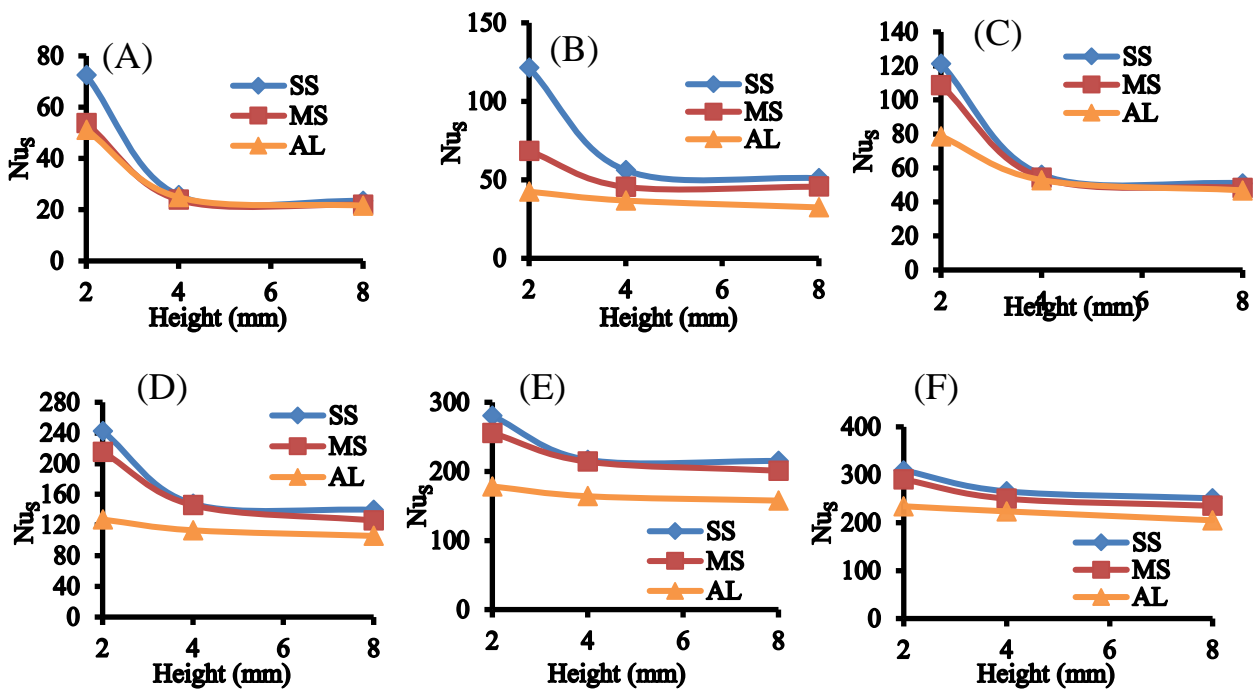


Fig. 3. Effect of nozzle height (H) on the Nu_s at air velocity (v) of 9.2 m/s for various nozzle diameters (A) 0.5 mm; (B) 1 mm; (C) 1.5 mm; (D) 2 mm; (E) 2.5 mm; (F) 3 mm.

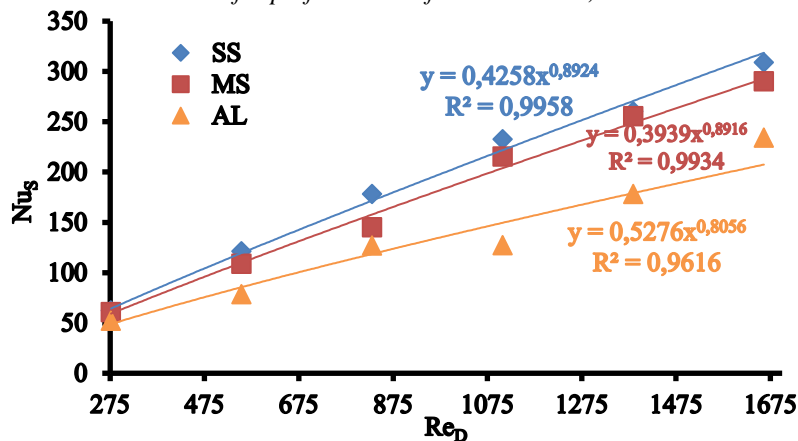


Fig. 4. Relationship between Re_D and the maximum Nu_s obtained (when $H = 2$ mm and $v = 9.2$ m/s)

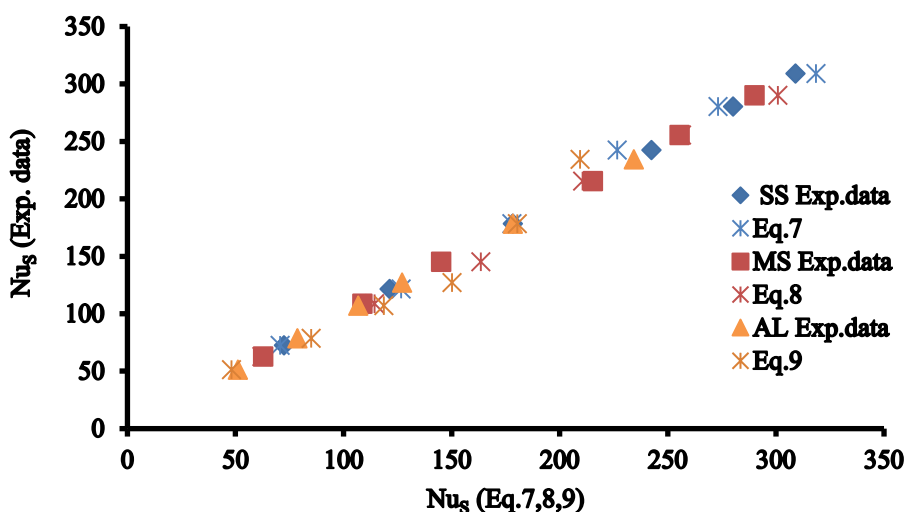


Fig. 5. Validation of experimental (Exp.) Nu_s data against empirical Nu_s data obtained from Eqs. 7, 8 and 9.

The Nu_s values obtained from these empirical correlations were plotted against the experimental values in Fig. 5. One could observe that the experimental values are closer to the empirical values derived from Eqs. 7, 8 and 9. The average deviation between the experimental and predicted values for SS, MS and AL were found to be 3.17%, 4.17% and 9.16%, respectively, and these deviations are well within the permissible error of 15% [6]. Thus, the empirical correlations developed in this study were validated and the best performing material among the three was SS.

CONCLUSIONS

Effects of forced convection heat transfer over three different horizontal flat plates in the stagnation region were investigated with an impinging air jet. The experiments carried out for different values of nozzle diameter, flow velocity, and nozzle height revealed that the stagnation Nusselt number is at the peak for the least nozzle location height for all nozzles albeit the variations in nozzle diameter and

air velocity. Higher air velocity with increased Reynolds number yielded better heat transfer performance. A new empirical correlation was derived for each target material and the predicted values were validated against the experimental data. Stainless steel plate showed evidently better heat transfer ability under the experimental conditions of this study.

REFERENCES

1. J. Ferrari, N. Lior, J. Slycke, *J. Mater. Process. Technol.*, **136**, 190 (2003).
2. H. Martin, *Adv. Heat Transfer*, **13**, 1 (1977).
3. K. Jambunathan, E. Lai, M. A. Moss, B. L. Button, *Int. J. Heat Fluid Flow*, **13**, 106 (1992).
4. C. D. Donaldson, R. S. Snedeker, *J. Fluid Mech.*, **45**, 281 (1971).
5. Y. J. Chou, Y. H. Hung, *J. Heat Transfer*, **16**, 479 (1994).
6. Z. H. Lin, Y. J. Chou, Y. H. Hung, *Int. J. Heat Mass Transfer*, **40**, 1095 (1997).
7. I. Sezai, L. B. Y. Aldabbagh, in: The effect of jet-to-jet spacing on the cooling performance of impinging

- K. Jeyajothi, P. Kalaichelvi: Heat transfer performance of stainless steel, mild steel and aluminium target plate ... jet arrays, Proc. 3rd Int. Conf. Comput. Heat Mass Transfer, Banff, Canada, 2003, p. 26.*
8. R. J. Goldstein, A. I. Behbahani, *Int. J. Heat Mass Transfer*, **25**, 1377 (1982).
 9. L. B. Y. Aldabbagh, I. Sezai, A. A. Mohamad, *J. Heat Transfer*, **125**, 243 (2003).
 10. S. Al-Sanea, *Int. J. Heat Mass Transfer*, **35**, 2502 (1992).
 11. M. Rady, E. Arquis, *Appl. Therm. Eng.*, **26**, 1310 (2006).
 12. S. C. Arjocu, J. A. Liburdy, *J. Heat Transfer*, **122**, 240 (2000).
 13. G. K. Morris, S. V. Garimella, R. S. Amano, *J. Heat Transfer*, **118**, 562 (1996).
 14. R. Viskanta, *Exp. Therm. Fluid Sci.*, **6**, 111 (1993).
 15. S. J. Downs, E. H. James, *ASME*, 87-HT-35 (1987).
 16. S. Polat, B. Huang, A. S. Mujumdar, W. J. M. Douglas, *Annu. Rev. Numer. Fluid Mech. Heat Transfer*, **2**, 157 (1989).
 17. F. F. Grinstein, E. Gutmark, T. Parr, *Phys. Fluids*, **7**, 148 (1995).
 18. R. J. Moffat, *J. Fluid Sci.*, **1**, 3 (1988).
 19. C. F. Ma, Q. Zheng, H. Sun, K. Wu, K. Horii, *Exp. Therm Fluid Sci.*, **17**, 238 (1998).
 20. J. N. B. Livingood, P. Hrycak, Lewis Research Centre, NASA TM X-2778, (1973).
 21. C. Meola, *Heat Transfer Eng.*, **30**, 221 (2009).
 22. S. E. Mahgoub, *Ain Shams Eng. J.*, **4**, 605 (2013).

ЕФЕКТИВНОСТ НА ТОПЛОПРЕНОСА НА ПЛАСТИНИ ОТ НЕРЪЖДАЕМА СТОМАНА, МЕКА СТОМАНА И АЛУМИНИЙ ЗА РАЗЛИЧНИ КОНФИГУРАЦИИ НА УДАРНА ВЪЗДУШНА ДЮЗА

К. Джеяджоти, П. Калайчелви*

Департамент по инженерна химия, Национален технологичен институт, Тиручирапали- 620015, Тамил Наду, Индия

Постъпила на 17 юли, 2018; коригирана на 3 август, 2018

(Резюме)

Описан е нов подход за сравняване на характеристиките на топлопренос при ударна струя върху равна повърхност от различен материал. Нагреваемите пластини са изготвени от неръждаема стомана, мека стомана и алуминий и са разположени на различни разстояния (от 2 до 8 mm) от дюзата с диаметър от 0.5 до 3 mm. Измерванията са проведени при точката на стагнация с използване на въздушна струя със скорост от 6.4 и 9.2 m/s. Основните характеристики на струйния удар върху повърхността могат да се илюстрират чрез прост експеримент, например, по метода на разпространението. Числото на Nusselt е пресметнато за различни стойности на струйното число на Reynolds и е установено, че се постига адекватно охлаждане на пластината, което се подобрява с нарастване на числото на Reynolds. Установено е също, че позицията на пластината е критична за оптималната ефективност при практическо приложение. Повишаването на скоростта на въздуха и на числото на Reynolds води до подобряване на топлопреноса, докато повишаването на височината на дюзата влошава ефективността в точката на стагнация. На основата на проведените експерименти са намерени три нови корелации.